Upper ocean mixing controls the seasonality of planktonic foraminifer fluxes and associated strength of the carbonate pump in the oligotrophic North Atlantic

K.H.Salmon[1], P. Anand[1], P.F. Sexton[1], M. Conte[2]

[1] Environment, Earth and Ecosystems, The Open University, United Kingdom

[2] Bermuda institute of Ocean Sciences, St Georges GE01, Bermuda

Abstract

Oligotrophic regions represent up to 75% of Earth's open-ocean environments. They are thus areas of major importance in understanding the plankton community dynamics and biogeochemical fluxes. Here we present fluxes of total planktonic foraminifera and eleven planktonic foraminifer species measured at the Oceanic Flux Program (OFP) time series site in the oligotrophic Sargasso Sea, subtropical western North Atlantic Ocean. Foraminifera flux was measured at 1500 m water depth, over two ~2.5 year intervals, 1998-2000 and 2007-2010. We find that foraminifera flux was closely correlated with total mass flux, carbonate and organic carbon fluxes. We show that the planktonic foraminifera flux increases approximately five-fold during the winter-spring, contributing up to ~40% of the total carbonate flux. This was primarily driven by increased fluxes of deeper dwelling globorotaliid species, which contributed up to 90% of the foraminiferal-derived carbonate during late winter-early spring. Interannual variability in total foraminifera flux, and in particular fluxes of the deep dwelling species (*Globorotalia truncatulinoides, Globorotalia hirsuta* and *Globorotalia inflata)*, was related to differences in seasonal mixed layer dynamics affecting the strength of the spring phytoplankton bloom and export flux, and by the

passage of mesoscale eddies. As these heavily calcified, dense carbonate tests of deeper dwelling species (3 times denser than surface dwellers) have greater sinking rates, this implies a high seasonality of the biological carbonate pump in oligotrophic oceanic regions. Our data suggest that climate cycles, such as the North Atlantic Oscillation, which modulates nutrient supply into the euphotic zone and the strength of the spring bloom, may also in turn modulate the production and flux of these heavily calcified deep-dwelling foraminifera by increasing their food supply, thereby intensifying the biological carbonate pump.

1. Introduction

Planktonic foraminifera (PF) comprise 23-56% of the total open marine calcite flux and thus exert an important control on global carbon cycling (Schiebel, 2002). They are used extensively in palaeoceanographic and palaeoclimatic reconstructions via utilisation of their species abundance and assemblage composition (e.g., Lutz, 2011; Sexton and Norris, 2011), geochemical signatures (e.g., Zeebe et al. 2008), shell mass (e.g., Barker and Elderfield, 2002) and in evolutionary and biogeographic studies (e.g. Sexton and Norris, 2008). However, gaps remain in our understanding of the controls on their spatial and temporal distribution in the upper water column. Following the early 1980s when sea surface temperatures (SSTs) were thought to dominantly control PF distributions and abundance (CLIMAP project members, 1994), a number of other environmental parameters have also been shown to exert influence on the distribution and abundance of PF, such as salinity (Kuroyanagi and Kawahata, 2004), productivity, nutrient availability (Schiebel, 2002, Northcote et al. 2005, Žarić et al. 2005; Storz et al. 2009; Sexton and Norris, 2011) and water column stability (Hemleben et al. 1989, Lohmann and Schweitzer 1990, King and Howard, 2003). It is thus imperative to better understand the environmental factors controlling modern-day PF abundance in order to produce accurate interpretations of palaeorecords based on PF assemblages.

The response of PF flux and species composition to environmental and/or oceanographic factors have been studied using plankton tow materials which can give information about living populations' species distribution and depth habitats within the upper ocean (Tolderlund and Be, 1971, Fairbanks et al., 1980; Schiebel 2002). However, temporal resolution is often limited when using plankton tows. The continuous time series records provided by sediment-traps allow a more complete

61 understanding of the seasonal and interannual changes in PF flux and can aid in
62 integrating living assemblages with the sedimentary record.
63
64 Earlier studies of planktonic foraminifer flux off Bermuda at the Seasonal Changes in
65 Foraminifera Flux (SCIFF) site (Figure 1) (Deuser et al. 1981, Hemleben et al. 1985,
66 Deuser 1987, Deuser and Ross 1989) were based on a bi-monthly sampling interval
67 and provide a general description of foraminifera flux, species composition and
68 seasonality. These studies found that PF >125μm comprise on average 22% of the
69 total calcium carbonate flux in the Sargasso Sea (Deuser and Ross 1989), although
70 this average underestimates the importance of the PF flux contribution during
71 different seasons. Here we utilise a higher resolution bi-weekly sediment trap time
72 series from the Oceanic Flux Program (OFP), ideal for studying the detailed response
73 of PF species flux to physical oceanographic changes because PF species lifespan is
74 approximately 2-3 weeks (Spero, 1998, Erez et al. 1991). These samples also benefit
75 from the availability of upper ocean hydrographic and biogeochemical data collected
76 at the nearby Bermuda Atlantic Time Series (BATS) site, as well as remote sensing
77 data, which allows us to evaluate the environmental factors that control the total
78 foraminifer flux as well as the response of individual species flux. Furthermore, we
79 assess the relative contribution of PF flux to regional carbonate export and explore the
80 implications of our findings for carbonate cycling in the oligotrophic North Atlantic.
81

2. Oceanographic Setting

The Sargasso Sea is located within the North Atlantic gyre, which is characterised by high temperatures and salinities, and weak, variable surface currents (Lomas et al. 2013 and references therein). The OFP and BATS sites are situated in a transition region between the northern eutrophic waters and the relatively oligotrophic subtropical convergence zone in the south (Steinberg et al. 2001 and references therein). Subtropical Mode Water (STMW) forms on the fringes, north of the gyre, owing to convective deep winter mixing and entrainment of nutrients and is characterized by temperatures of 17.8-18.4ºC and salinities of ~36.5 +/- 0.05 (Bates et al. 2002), typically occurring between ~250-400 m water depth (Bates, 2007).

The hydrography and biogeochemistry of the area have been summarized by Michaels and Knap (1996), Steinberg et al. (2001), Lomas et al. (2013) and references therein. In the absence of large changes in salinity, the 10°C seasonal change in surface temperatures driven by solar insolation, controls the shoaling and erosion of the mixed layer, which reaches a maximum of 250-400m in late winter, increasing vertical mixing and entraining nutrient-rich waters. The depth of mixing determines the strength of seasonal particulate flux, nutrient concentrations and primary production during the subsequent spring bloom (Michaels and Knap, 1996, Steinberg et al., 2001). With the onset of seasonal stratification in late February-March, a spring bloom develops when phytoplankton biomass and particulate organic carbon standing stocks are maximal. As seasonal stratification intensifies, a nutrient-depleted, shallow surface mixed layer develops which is underlain by a subsurface chlorophyll maximum at approximately 80-100m depth. Strong stratification in summer and

autumn results in low vertical mixing that limits nutrient availability and primary production. Seasonal cooling in late autumn results in erosion and gradual deepening of the mixed layer, with renewed nutrient entrainment into the euphotic zone and an increase in primary production. Mesoscale physical variability in this area is the dominant method of nutrient transport (McGillicuddy et al., 1998). In particular, passage of cyclonic and mode water eddies may lead to nutrient entrainment which generates short-lived phytoplankton blooms and community restructuring (Wiebe and Joyce, 1992, Olaizola et al., 1993, McNeil et al., 1999, Letelier et al., 2000, Seki et al., 2001, Sweeny et al., 2003) which could, in turn, impact higher trophic levels such as planktonic foraminifera. In addition, these blooms often result in short-lived, episodic periods of enhanced export fluxes of labile organic material to depth (Conte et al. 1998, 2003, 2014).

3. Materials and methods

3.1 The OFP Sediment trap time-series

The OFP mooring is located at 31° 50'N, 64° 10'W, about 55 km southeast of Bermuda at 4200m water depth (Figure 1). Three Mark VII Parflux sediment traps (McLane Labs, Falmouth, MA) are deployed at depths of 500 m, 1500 m and 3200 m. The traps (0.5 m^2 surface area) are programmed to collect a continuous bi-weekly time-series of the particle flux. Collected samples were processed according to Conte et al. (2001) and split into < 125 μm, 125-500 μm, 500-1000 μm and >1000 μm size fractions. We analyzed foraminifera in the 125-500 μm and 500-1000 μm size fractions of 1500m trap samples collected during two time periods: 1998-2000 and 2008-2010 (109 samples total). We selected the two equivalent 2.5 year intervals a decade apart to generate a bi-weekly resolved time-series which would enable assessment of seasonality as well as interannual variability. Our analyses focused on eleven species that fall within three general groupings: i) surface dwelling species living within the upper 50 m water column (*Globigerinoides ruber var*. white/pink, *Globigerinella siphonifera, Globigerinoides sacculifer*), ii) intermediate dwelling species living in the ~50-200 m depth range (*Orbulina universa, Globigerinoides conglobatus, Neogloboquadrina dutertrei, Pulleniatina obliquiloculata*) and iii) deep dwelling species (or species that are thought to calcify over a large depth range) living in the ~100-800 m depth range (*Globorotalia inflata, Globorotalia crassaformis, Globorotalia truncatulinoides, Globorotalia hirsuta*). Our assignments of the depth habitats were based on measured species depth distributions and/or inferred distributions based on oxygen isotopic composition (Fairbanks et al., 1980, Anand et

al., 2003). The temporal offset between the foraminiferal species fluxes reaching the trap at 1500m depth versus the timing of these species' growth in overlying waters will vary depending on habitat depths and individual species' sinking rates (Takahashi and Bé, 1984). A surface-dwelling *G. ruber* living at 25 m depth may sink at ~198 m day^{-1}, taking ~7 days to reach the 1500 m trap, whereas a more heavily calcified deeper-dwelling species such as *G. inflata* may sink ~504 m day^{-1}, taking only ~3 days to reach the 1500 m trap. These fast sinking rates are much shorter than the typical lifespans of PF and are thus not anticipated to cause any offset between the hydrographic and sediment trap flux data (Honjo and Manganini, 1993).

On average, ~440 tests were counted in each sample fraction. To generate the flux data, counts of total and individual foraminifera species in the sample aliquots for each size fraction was converted to total counts per sample fraction and then the totals for the two fractions were combined (i.e. total planktonic foraminifera between 125-1000 um in size). Total counts were then scaled for the processing split (60%) and converted to flux (tests m^{-2} d^{-1}).

3.2 BATS and remote sensing data

The BATS site ($31^0$40'N, $64^0$10'W) is located just south of the OFP mooring (Figure 1). Monthly hydrographic and biogeochemical data collected by the BATS time-series was obtained from the BATS website (http://bats.bios.edu). Mixed layer depth (MLD) was available from Lomas et al. (2013) and was calculated from CTD profiles using the variable sigma-*t* criterion equivalent to a 0.2°C temperature change (Sprintall and Tomczak, 1992). The mesoscale eddy field was assessed using

171 interpolated data on sea surface anomaly available from the CCAR Global Historical

172 Gridded SSH Data Viewer

173 (http://eddy.colorado.edu/ccar/ssh/hist_global_grid_viewer).

174 **4.1. Total planktonic foraminiferal fluxes**

175

176 ***4.1.1. In relation to other mass fluxes***

177

178 The seasonal cycle and interannual variability of the PF flux at 1500m depth is highly
179 correlated with that of the total mass, carbonate and organic carbon fluxes. All fluxes
180 are strongly characterized by an abrupt spring maximum during February-April,
181 which varies significantly on an interannual basis (Figure 2). For example, the spring
182 PF flux peak ranged from a low of 400 tests m^{-2} day^{-1} in 2008, coinciding with
183 minimal spring mass fluxes, to a high of 900 tests m^{-2} day^{-1} in 2009, coinciding with
184 an extreme peak in spring mass fluxes. All fluxes typically drop to a minimum over
185 the summer months (May-August) and remain low until the following spring bloom.
186 During these minima, the PF flux generally amounts to <200 tests/m^2/day. In some
187 years (e.g. 2009 and, to a lesser extent, 2008), the PF flux displays a smaller, but
188 distinct second peak in the months September-October. This secondary autumn peak
189 can also be seen in the mass flux and carbonate flux in 2009 but is absent in the
190 organic carbon flux. Over the entire record, the correlation between PF flux and mass,
191 carbonate and organic carbon flux is 0.65, 0.64 and 0.55, respectively.

192

193 ***4.1.2 Relative to upper ocean hydrography***

194

195 In Figure 3 we compare interannual variations in bi-weekly resolved total PF flux to
196 ~monthly resolved changes in key upper ocean hydrographic parameters, measured at
197 the BATS site. PF flux exhibits an inverse relationship with seasonal variations in sea
198 surface temperatures (SST) and reaches a maximum when SST is coolest in January-

March (Figure 3a). Of note, is the particularly large and prolonged PF bloom in 2010, which coincided with a cyclonic eddy that passed through the area causing the lowest SSTs on record for this site ~18.9°C (Figure 3a-b).

Sea level anomaly (SLA) provides information about eddies passing through the area (Figure 3b). A negative anomaly is associated with cyclonic eddies and a positive anomaly associated with anticyclonic and mode water eddies. The SLA data show that the particularly high and prolonged PF fluxes, total mass flux and organic carbon flux in spring 2009 and 2010 coincided with the passage of cold, cyclonic eddies (Figure 2), which enhance nutrient upwelling into the euphotic zone.

The annual and interannual PF flux is in phase with the deepening and shoaling of the mixed layer depth (MLD) (Figure 3c) and with chlorophyll *a* concentrations (Figure 3d). The seasonal PF flux maximum coincides with the chlorophyll *a* maximum (which is used here as a proxy for the spring phytoplankton bloom) and the organic carbon flux from 200m, which represents organic carbon export from surface productivity (Figure 3e), and the deepest MLD during February-March. During April-May, the MLD shoals back towards the surface coinciding with decreasing chlorophyll *a* concentrations and PF flux. The strong correlations between the seasonality in PF flux and that of primary production and export is demonstrated by the regressions between total PF flux and chlorophyll *a* concentration (Figure. 4a) and the 1500m mass flux (Figure. 4b). During the winter-spring period the magnitude of PF flux generally follows the evolution in MLD and is maximal when the MLD is maximal (Figure. 4c). However, when the mixed layer depth shoals to <80 m during the low productivity period in late spring and summer, this correlation is not significant (Figure. 4d).

225 **4.2 Planktonic foraminifera species fluxes**

226

227 In general, all planktonic foraminifera, and especially deeper dwelling species, show
228 strong, consistent seasonal variance (Figures 5-7). Our results demonstrate a clear
229 depth progression towards more pronounced seasonality in the deeper species,
230 compared to a larger intra-seasonal variability in the surface and intermediate
231 dwellers. In addition, the deep dwelling PF species exhibit repeatable species
232 successions throughout the winter and early spring (Figure 8, Table 1). Figure 8
233 shows that *Globorotalia truncatulinoides* dominates the flux of deeper dwellers, and
234 thrives each December, reaching a maximum during January. *G. truncatulinoides* is
235 then followed by *G. hirsuta*, *G. crassaformis*, and *G. inflata* which all peak between
236 March and April. *G. truncatulinoides* displays large interannual variability (Table 1),
237 ranging from lows of ~4000 tests/m^2/year in 2009-2010 to highs of up to ~14 000
238 tests/m^2/year in 1999-2000 (Figure 6). The remaining deeper dwellers (*Globorotalia*
239 *hirsuta, Globorotalia inflata, Globorotalia crassaformis*) also vary on an interannual
240 basis. Figure 7 and Table 1 show that the largest fluxes of deeper dwelling species
241 occurred during the winter/spring of 1999-2000 and 2008-2009. Using shell weights
242 from this study averaged with shell weights (125-1000um) measured by Deuser,
243 (1987) and Deuser and Ross, (1989), we estimate that PF flux contributes up to ~40%
244 of the total carbonate flux during winter-spring but <10% during summer (Figure 9a).
245 Deeper dwelling species account for 60-90% of PF carbonate flux (Figure 9b) and up
246 to 37.5% of the total carbonate flux (e.g. during the winter-spring of 2000) (Figure 9c).

247
248

5. Discussion

The controls on PF flux in the Sargasso Sea was first introduced by Bé, (1960) and later developed by Tolderlund and Bé, (1971) who suggested that PF flux is dominantly controlled by the availability of their food phytoplankton. Thus, the environmental factors controlling PF flux should be closely aligned with the factors controlling phytoplankton productivity and export flux.

5.1 Environmental controls on PF fluxes

5.1.1. Depth of the mixed layer

Previous studies suggest that increased chlorophyll concentrations and larger phytoplankton abundances occur when the MLD deepens (Townsend et al. 1994, Waniek, 2003, Nelson et al. 2004) and the amplitude and timing of MLD deepening determines the size of the following spring bloom (Menzel and Ryther, 1961, Michaels et al. 1994). Here, we also observe a simultaneous seasonal peak in chlorophyll *a* and maximum depth of the MLD, as observed by previous studies at BATS (Steinberg et al. 2001, Cianca et al. 2012), the timing and amplitude of which coincides with the maximum PF flux (Figure. 3c, d). Similarly, seasonal changes in mixed layer depth are closely associated with changes in foraminifer production (Thunell and Reynolds, 1984, Sautter and Thunell, 1989, Pujol and Vergnaud Grazzini 1995, Schmuker and Sciebel 2002) and chlorophyll *a* concentrations (King and Howard, 2003, 2005) in other ocean basins. Siegel et al. (2002) proposed that south of 40°N, the initiation and extent of the spring bloom is dominantly limited by

274 nutrients, and this is supported by the simultaneous increase in phytoplankton
275 concentrations with mixing depth at BATS (Treusch et al. 2012). Vertical mixing in
276 late winter and spring distributes nutrients into the euphotic zone to support the spring
277 phytoplankton bloom, causing the consequent seasonal peak in export fluxes of
278 organic carbon, to fuel symbiont-barren foraminifera production (Figure. 2d). In
279 contrast, no correlation exists between PF flux and MLD during the late spring to
280 autumn when the mixed layer fails to penetrate the minimum depth of the deep
281 chlorophyll maximum layer (~80m), where many species of planktonic foraminifera
282 reside in association with other zooplankton and algal cells (Fairbanks and Wiebe,
283 1980) (Figure 4d). This is also the depth of the nitricline where nitrate concentrations
284 > 0.1 umol kg^{-1}, (Sciebel et al. 2001).
285
286 The majority of the increased PF flux in the winter-spring is driven by increased
287 fluxes of deeper dwelling species, in particular *G. truncatulinoides* and *G. hirsuta*
288 (Figure. 9b). These species are symbiont-barren and rely on the flux of phytodetritus
289 and other labile organic carbon as a food source from the spring phytoplankton bloom
290 (Hemleben et al. 1989). The discrepancy in timing of peaks between the deeper
291 dwelling species (Figure 8) is likely due to subtle changes in phytoplankton
292 succession related to the species' diets (Deuser and Ross, 1989, Hemleben et al. 1989).
293 Overall, the seasonal PF species succession is broadly similar to previous
294 observations from 1959-63 and 1978-84 (Tolderlund and Bé, 1971, Deuser 1987,
295 Deuser and Ross, 1989) which suggests that despite long-term environmental change,
296 species seasonality have remained consistent over the past 50 years.
297

298 The correlation observed here between the seasonality in the PF flux, chlorophyll *a*
299 concentration and mass flux at 1500m (Figure 4 a and b) clearly demonstrates that the
300 seasonality of non symbiont-bearing foraminifera, such as the globorotaliids is
301 controlled by phytoplankton production and the export flux of phytodetritus to depth.
302 As these globorotaliids are up to three times denser than surface species (unpublished
303 data), their sinking rates are significantly higher than those of other species. Thus,
304 increased production by these species can accelerate the transfer of carbonate from
305 surface to deep-ocean, thereby strengthening the carbonate pump.
306
307 In contrast, the surface-dwelling symbiont-bearing foraminifera have lifecycles which
308 strongly benefit from stratified surface waters and shallow mixed layers in order to
309 photosynthesise allowing them to succeed in low nutrient conditions (Hemleben et al.
310 1989). Surface dwellers generally calcify in late summer when sea surface
311 temperatures are at a maximum and dinoflagellates are abundant (Tolderlund and Bé,
312 1971). We thus conclude that the depth and structure of the mixed layer plays an
313 important role in regulating PF species flux by controlling the abundance and timing
314 of their food availability throughout the seasonal cycle.
315
316 ***5.1.2. MLD deepening and shoaling rates***
317
318 Current models based on the light-limited higher latitudes (Waniek, 2003; Mao, Y.,
319 2013- personal communication), suggest that if the MLD shoals early and slowly, the
320 consequent bloom will be long and weak compared to if the MLD shoals late and
321 quickly, which causes a short and sharp bloom. At our subtropical study site, the
322 spring bloom is predominantly limited by nutrient input into the euphotic zone, which

323 is determined by the depth of the mixed layer. Increased heat loss and wind stress
324 leading to higher convective mixing during the winter months controls the rate of
325 deepening of the mixed layer, which is strongly correlated to the maximum MLD
326 reached ($r^2 = 0.88$) (Figure 10a). Years with faster deepening rates have deeper
327 mixed layers and hence larger spring blooms (e.g. winter 2009), whereas slow
328 deepening rates cause shallower mixed layers and smaller spring blooms. There is
329 also some evidence that light-limitation could be a secondary control on the peak
330 productivity of the spring bloom at this site (Dutkiewicz et al. 2001, Lomas et al. 2009,
331 Cianca et al. 2012) as the euphotic zone extends to ~100m (Steinberg et al. 2001) and
332 a faster shoaling rate during the spring could control could concentrate the food
333 available for symbiotic-foraminifera in the euphotic zone, resulting in a larger PF flux.
334
335 To test whether the rates of mixed layer deepening in early winter and of shoaling in
336 spring affect the PF flux, we computed a mixed layer dynamics index, D_r/S_r, which is
337 the ratio of the rate of deepening to the rate of shoaling and compared this to the
338 integrated PF flux (Table 2). The D_r/S_r ratio never exceeds 1, indicating that the
339 shoaling rate always exceeds the deepening rate. For all the years studied, there is a
340 strong inverse relationship between the integrated PF flux over the duration of spring
341 bloom, and the D_r/S_r ratio (Figure 10b, $r^2 = 0.93$). This relationship is also present in
342 the maximum in chlorophyll *a* concentration and the D_r/S_r ratio (Figure 10c, $r^2 = 0.76$).
343 This correlation indicates that when the MLD shoals more quickly during spring
344 stratification (lower D_r/S_r ratio), the chlorophyll *a* concentrations and PF flux are
345 higher, as supported by a strong correlation ($r^2 = 0.87$) between shoaling rate and
346 integrated PF flux (Figure 10d).
347

348 Years where the shoaling rate is twice as quick as the deepening rate (e.g. winters
349 1997, 2008, and 2009) have average D_r/S_r ratios, average-length blooms and PF flux
350 (~30 tests/m^2/day, Table 2). Years with comparatively equal rates of shoaling and
351 deepening (e.g. winter 2007) have larger D_r/S_r ratios, longer and slower blooms with
352 shallower MLDs and small PF fluxes. Years when the shoaling rate is much quicker
353 than deepening rate e.g. winter 1999 have the smallest D_r/S_r ratios and shorter, sharper
354 blooms with greater numbers of intermediate thermocline dwelling species such as *N.*
355 *dutertrei, P. oblquiloculata, G. siphonifera*, suggesting that when the rate of shoaling
356 is higher the seasonal thermocline is nearer to the surface for longer, which is
357 beneficial for these symbiont-bearing and symbiont-facultative species. The PF
358 fluxes were large (and prolonged) respectively in winter 2008-09 and 2009-10 despite
359 having average D_r/S_r ratios but were probably enhanced by additional factors
360 discussed in the next section.
361
362

363 ***5.1.3 Eddies***

364

365 The negative sea level anomalies in spring of 2009 and 2010 indicate that the large
366 (and in 2010 prolonged) PF fluxes in these years were clearly associated with the
367 passage of cyclonic eddies (Figure 3b). Eddy pumping of nitrate into the euphotic
368 zone has been shown to significantly increase new production (Oschlies and Garçon,
369 1998, Oschlies, 2002). Cianca et al. (2007) estimate that eddy pumping contributes
370 ~50% of the nutrient input into the euphotic zone in the Sargasso Sea. Studies at the
371 BATS site have demonstrated the influence of cyclonic and mode water eddies in
372 promoting phytoplankton blooms and increased secondary production (Eden et al.,
373 2009, McGillicuddy et al. 2007, Goldthwait and Steinberg, 2008, McGillicuddy et al.,
374 1999, Sweeney et al., 2003, Lomas et al. 2013, Cianca et al. 2012) and therefore
375 affecting PF food availability and quality (Schmuker and Schiebel, 2002). Previous
376 studies have found higher fluxes of certain PF species such as *Globigerinita glutinata*
377 associated with cyclonic eddy structures in the Caribbean Sea (Schmuker and
378 Schiebel, 2002) and North Atlantic (Beckman et al. 1987), also in conjunction with
379 upwelling frontal regions in the Mexican Pacific (Machain-Castillo et al. 2008) and
380 deep mixed layers during winter in the Mediterranean (Pujol and Vergnaud Grazzini,
381 1995). Here we observe a similar response during the passage of a cyclonic eddy in
382 spring 2009, particularly for deeper dwelling species. In fact, the largest PF flux
383 observed over the entire record was associated with this eddy passage, even though
384 the maximum MLD and D_r/S_r were modest (Table 2). Similarly, the mass and organic
385 carbon flux measured during passage of this eddy (Figure. 2b-d) were the highest
386 fluxes measured over the last 25 years of the OFP time-series, indicating that the
387 conditions in this eddy promoted an extremely large export flux to fuel the production

388 of deep dwelling foraminifera species such as *G. truncatulinoides, G. hirsuta,* and
389 especially *G. inflata* which all experienced higher seasonal fluxes in 2009 (Figure 7).
390
391 This observation is consistent with an exceptionally large increase in the flux of *G.*
392 *truncatulinoides* (> 600 tests m^{-2} day^{-1}) seen at the OFP traps during the spring of
393 2007, which was also influenced by the passage of a productive cyclonic eddy (Fang
394 et al. 2010, Conte et al. 2014). Both the 2007 and 2009 eddies occurred between
395 January-March during the seasonal flux of the deeper dwellers (Figure 7),
396 underscoring the importance of the timing of eddy passage in enhancing PF flux. The
397 influence of eddies here is similar to observations from the Eastern Mediterranean
398 where increased numbers of grazing species such as *G. truncatulinoides* and *G. inflata*,
399 have been found in association with eddy structures and deep mixed layers (Pujol and
400 Vergnaud Grazzini, 1995). These findings suggest that productive cyclonic eddies,
401 when co-occurring with deep MLDs, act to enhance the existing seasonal abundance
402 of deeper dwelling species through mixing of the water column, which aids their
403 annual reproductive migration in addition to increasing food supply.
404
405 Along with the timing of the eddy passage, our observations also suggest that the PF
406 flux response is dependent on whether the eddy is intensifying or weakening. For
407 instance, both cyclonic eddies in 2009 and 2010 intensified over the spring bloom
408 (Figure 3b) eliciting a large biological response indicated by elevated subsurface Chl-
409 *a* concentrations and increased PF flux. In contrast, the cyclonic eddy in winter 2007-
410 08 was weakening over the spring bloom and therefore elicited no PF flux response.
411 Recent studies have found that eddies which are a minimum of 1-2 months in duration
412 are more likely to induce a larger biological response (Mouriño-Carballido and

McGillicuddy, 2006, Sweeny et al. 2003). Our observations also suggest that eddies need to be present for at least a month to elicit responses in the flux of PF which have minimum lifecycles of two weeks. For instance, in winter 1998-99 a cyclonic eddy passed over the sediment trap site in only one month and elicited no biological response, compared to cyclonic eddies in 2009 and 2010, which both remained over the site for a minimum of 2-3 months and elicited large biological responses (Figure 3b). These findings suggest that cyclonic eddies which intensify over the spring bloom and last for 1-3 months can elicit a significant biological response and increased PF flux.

6. Implications

Our results show that environmental factors and mesoscale eddy variability play an important role in regulating the planktonic foraminifera fluxes, by regulating the MLD and consequent magnitude of the spring bloom and biological export flux.

An overarching climatological variable affecting this region especially is the North Atlantic Oscillation (NAO), which exerts a strong influence on air temperature, storminess, heat loss, winter mixed layer depth, and, therefore, nutrient injection into the upper ocean during the winter months (Bates, 2012, Bates and Hansell, 2004, Rodwell et al. 1999). Modelling studies have shown that when the NAO is in its low phase, i.e. negative NAO (e.g. winter 2010), there is increased heat loss that intensifies convective mixing and results in enhanced nutrient upwelling into the euphotic zone to support primary production (Oschlies, 2001). The NAO influence on upper ocean productivity and biogeochemical fluxes is demonstrated by the inverse correlation between the wintertime (NDJF) NAO index and the deep particulate nitrogen flux in the OFP traps over a thirty-year period (Conte and Weber, 2014) and increased primary productivity in negative wintertime NAO phases (Lomas et al. 2010). If convective mixing and nutrient entrainment into the euphotic zone is stronger during negative NAO years, this could serve to modulate PF flux, and therefore carbonate flux, on decadal timescales. When we compare PF fluxes covering a range of NAO indexes, from this study using the 1500m trap to the 3200m trap between 1978-84 (Deuser and Ross, 1989, Deuser, 1987), we find a weak inverse correlation between total PF flux and (DJFM) NAO index in-phase (not significant), but we do find a significant inverse correlation with a (DJFM) NAO with a 1-year lag

449 ($p < 0.005$) (Figure 11). Cianca et al. (2012) showed that their correlation between
450 winter NAO and total Chlorophyll *a* at BATS improved when applying a +1 year time
451 lag, but still remained insignificant. They attributed this to variability in the
452 subtropical mode water, which can laterally advect nutrients on interannual timescales
453 (Palter et al. 2005, Patara et al. 2011). We acknowledge that additional longer-term
454 data is needed to test the mechanism behind this correlation, but our results suggest
455 that changes in NAO status and/or mesoscale eddy frequency could significantly
456 modulate planktonic foraminifera flux and export flux from the surface ocean on
457 interannual timescales.
458
459 This study shows that the productivity of the dominant deep dwelling species *G.*
460 *truncatulinoides* and *G. hirsuta* is especially responsive to interannual variability in
461 overlying surface water conditions and especially to the transient high production/flux
462 events that are associated with the passage of productive cyclonic eddies that coincide
463 with their seasonal spring production peak. Our data show that deeper dwelling
464 species can account for up to ~90% of the total PF carbonate flux, representing up to
465 ~40% of the total carbonate flux during winter-spring at the OFP site. Changes in
466 NAO status, which modulates nutrient supply into the euphotic zone and the strength
467 of the spring bloom, also may in turn modulate the production and flux of these
468 heavily calcified deep-dwelling foraminifera by increasing their food supply, thereby
469 intensifying the carbonate pump.
470

7.0. Conclusions

Our study demonstrates that the interannual variability in planktonic foraminifera flux can be linked to the MLD and the rate of deepening/shoaling of the mixed layer associated with nutrient injection into the euphotic zone. We find that higher PF fluxes coincide with deeper MLDs, especially when combined with cyclonic eddy-induced nutrient upwelling. In particular, the production of the dominant deep dwelling species *G. truncatulinoides* and *G. hirsuta* is shown to be particularly responsive to interannual variability in overlying surface water conditions and especially to the transient high production/flux events that are associated with productive cyclonic eddies. These species dominate the major late winter-early spring pulses of foraminifera and have higher sinking rates than surface dwelling species because they are up to three times denser (unpublished results). We suggest deeper-dwelling species strengthen the carbonate pump by accelerating the transfer of carbonate from surface to deep ocean and contribute up to 40% of the contemporaneous peak in total carbonate export fluxes. It follows that any increase in fluxes of these deep-dwellers arising from climate-induced changes in winter-spring mixed layer dynamics will also increase the average sinking rate of foraminiferal carbonate and intensify the overall carbonate pump. Our findings suggest that the North Atlantic Oscillation, via its influence on mixed layer depth, nutrient upwelling, phytoplankton production and export flux may also serve to modulate the foraminiferal component of the carbonate pump in the subtropical North Atlantic.

Acknowledgements

We would like to thank two anonymous reviewers for their time and constructive comments that helped improve the manuscript. This research was funded through the U.K. Ocean Acidification Research Program by Natural Environment Research Council grant to P. Anand and P. Sexton (grant NE/I019891/1). We acknowledge the National Science Foundation for its support of the Oceanic Flux Program time-series (most recently by grant OCE-1234292) and the Bermuda Atlantic Time Series (most recently by grant OCE-0801991). We thank Mike Lomas for providing MLD data and Yolanda Mao for providing insights and useful discussion on the data. P.A. is also thankful to Werner Deuser for communication regarding published data.

507 **References**

508 Anand P., Elderfield, H, Conte, M.H., 2003. Calibration of Mg/Ca thermometry in
509 planktonic foraminifera from a sediment trap time series. Paleoceanography, 18,
510 1050, doi:10.1029/2002PA000846.
511
512 Barker, S., Elderfield, H., 2002. Foraminiferal calcification response to Glacial-
513 Interglacial changes in Atmospheric CO_2. Science, 297, 833-836.
514
515 Bates N.R., Pequignet, A.C., Johnson, R.J., Gruber, N., 2002. A short-term sink for
516 atmospheric CO_2 in the subtropical mode water of the North Atlantic Ocean. Nature,
517 420, 489-493.
518
519 Bates, N.R., Hansell, D.A., 2004. Temporal variability of excess nitrate in the
520 subtropical mode water of the North Atlantic Ocean. Marine Chemistry, 84, 225-241.
521
522 Bates, N.R., 2007. Interannual variability of the oceanic CO2 sink in the subtropical
523 gyre of the North Atlantic Ocean over the last 2 decades. Journal of Geophysical
524 Research, 112, C09013, doi:10.1029/2006JC003759
525
526 Bates, N.R., 2012. Multi-decadal uptake of carbon dioxide into subtropical mode
527 water of the North Atlantic Ocean. Biogeosciences, 9, 2649-2659.
528
529 Bé, A.W.H., 1960. Ecology of Recent planktonic foraminifera, Part 2- Bathymetric
530 and seasonal distributions off Bermuda. Micropaleontology 6, no. 4, 373-392, text-
531 figs, 1-19
532
533 Beckman, A., Auras, A., Hemleben, C., 1987 Cyclonic cold-core eddy in the eastern
534 North Atlantic, 111. Zooplankton. Marine Ecology Progress Series, 39, 165-173.
535
536 Cianca, A., Godoy, J.M., Martin, J.M., Perez-Marrero, J., Rueda, M.J., Llinás, O.,
537 Neuer, S., 2012 Interannual variability of chlorophyll and the influence of low-

frequency climate modes in the North Atlantic subtropical gyre, Global Biogeochemical Cycles, 26, doi:10.1029/2010GB004022.

CLIMAP Project Members, 1994, Climap 18k Database: IGBP PAGES/World Data Center-A for Paleoclimatology Data Contribution Series, v. 94-001.

Conte, M.H., Weber, J.C., Ralph, N., 1998. Episodic particle flux in the deep Sargasso Sea: an organic geochemical assessment. Deep-Sea Research I 45, 1819-1841.

Conte, M.H., Ralph, N., Ross, E.H., 2001. Seasonal and interannual variability in deep ocean particle fluxes at the Oceanic Flux Program (OFP)/Bermuda Atlantic Time Series (BATS) site in the western Sargasso Sea near Bermuda. Deep-Sea Research II, 48, 1471-1505.

Conte, M.H., Dickey, T.D., Weber, J.C., Johnson, R.J., Knap, A.H., 2003. Transient physical forcing of pulsed export of bioreactive organic material to the deep Sargasso Sea. Deep-Sea Research I, 50, 1157-1187.

Conte, M.H., Weber, J.C., 2014. Particle flux in the deep Sargasso Sea: The 35-year Oceanic Flux Program time series. Oceanography, 27, 142-14.

Deuser, W.G., 1987. Seasonal variations in isotopic composition and deep-water fluxes of the tests of perennially abundant planktonic foraminifera of the Sargasso Sea: Results from sediment-trap collections and their paleoceanographic significance. Journal of Foraminiferal Research, 17, 14-27.

Deuser, W.G., Ross, E.H., Anderson, R.F., 1981. Seasonality in the supply of sediment to the deep Sargasso Sea and implications for the rapid transfer of matter to the deep ocean, Deep-Sea Research, 28A, 495-505.

569 Deuser, W.G., Ross, E.H., 1989. Seasonally abundant planktonic foraminifera of the
570 Sargasso Sea: Succession, deep-water fluxes, isotopic composition, and
571 paleoceanographic implications, Journal of Foraminiferal Research, 19, 268-293.
572
573 Dutkiewicz, S., Follows, M., Marshall, J., Gregg, W.W., 2001 Interannual variability
574 of phytoplankton abundances in the North Atlantic, Deep-Sea Research II 48, 2323-
575 2344.
576
577 Eden, B.R., Steinberg, D.K., Goldthwait, S.A., McGillicuddy, Jr, D.J., 2009.
578 Zooplankton community structure in a cyclonic and mode-water eddy in the Sargasso
579 Sea. Deep-Sea Research I, 56, 1757-1776.
580
581 Erez, J., Almogi-Labin, A., Avraham, S., 1991. On the life history of planktonic
582 foraminifera: lunar reproduction cycle in *Globigerinoides sacculifer* (Brady),
583 Paleoceanography, 6, 295-306
584
585 Fairbanks, R.G., and Wiebe, P.H., 1980 Foraminifera and Chlorophyll Maximum:
586 Vertical Distribution, Seasonal Succession, and Paleoceanographic Significance,
587 Science, 209, 1524-1526
588
589 Fairbanks, R.G., Wiebe, P.H., Bé, A.W., 1980. Vertical distribution and isotopic
590 composition of living planktonic foraminifera in the western North Atlantic. Science,
591 207, 61-63
592
593 Fang, J., Conte, M.H., Weber, J.C., 2010. Influence of physical forcing on
594 seasonality of biological components and deep ocean particulate flux in the Sargaddo
595 Sea. Eos, Transactions American Geophysical Union 91(26), Ocean Sciences
596 Meeting Supplement, Abstract BO24B-02.
597
598 Goldthwait, S., Steinberg, D.K., 2008. Elevated biomass of mesozooplankton and
599 enhanced fecal pellet flux in cold-core and mode-water eddies in the Sargasso Sea.
600 Deep Sea Research, 55, 1360-1377.

Hemleben, C., Spindler, M., Anderson, O.R., 1989. Modern Planktonic Foraminifera. Springer, New York, 363pp.

Honjo, S., and Manganini, S.J., 1993. Annual biogenic particle fluxes to the interior of the North Atlantic Ocean; studied at 34ºN 21ºW and 48ºN 21ºW. Deep Sea Research I, 40, 587-607.

King, A.L., and Howard, W.R., 2003 Planktonic foraminiferal flux seasonality in Subantarctic sediment traps: A test for paleoclimate reconstructions, Paleoceanography, 18, doi:10.1029/2002PA000839

King, A.L., Howard W.R., 2005 $\delta^{18}O$ seasonality of planktonic foraminifera from Southern Ocean sediment traps: Latitudinal gradients and implications for paleoclimate reconstructions, Marine Micropaleontology, 56, 1-24.

Kuroyanagi, A., Kawahata, H., 2004. Vertical distribution of living planktonic foraminifera in the seas around Japan. Marine Micropaleontology, 53, 173-196. doi:10.1016/j.marmicro.2004.06.001

Letelier, R.M, Karl, D.M., Abbott, M.R., Flament, P., Freilich, M., Lukas, R., Strub, T., 2000. Role of late winter mesoscale events in the biogeochemical variability of the upper water column of the North Pacific Subtropical Gyre. Journal of Goephysical Research, 105, 28 723-28 740. Correction in Journal of Goephysical Research, 106, 7181-7182.

Lohmann, G.P., Schweitzer, P.N., 1990. *Globorotalia truncatulinoides'* Growth and chemistry as probes of the past thermocline: 1. Shell size. Paleoceanography, 5, 55-75.

Lomas, M.W., Lipschultz, F., Nelson, D.M., Krause, J.W., Bates N.R., 2009

634 Biogeochemical responses to late winter storms in the Sargasso Sea I- Pulses of
635 primary and new production, Deep-Sea Research I, 56, 843-860.

636
637 Lomas, M.W., Bates, N.R., Johnson, R.J., Knap, A.H., Steinberg, D.K., Carlson, C.A.,
638 2013. Two decades and counting: 24-years of sustained open ocean biogeochemical
639 measurements in the Sargasso Sea. Deep-Sea Research II, 93, 16-32.
640
641 Lutz, B.P., 2011. Shifts in North Atlantic planktic foraminifer biogeography and
642 subtropical gyre circulation during the mid-Piacenzian warm period. Marine
643 Micropaleontology, 80, 125-149.
644
645 Machain-Castillo, M.L., Monreal-Gómez, M., Arellano-Torres, E., Merino-Ibarra, M.,
646 González-Chávez, G., (2008) Recent planktonic foraminiferal distribution patterns
647 and their relation to hydrographic conditions of the Gulf of Tehuantepec, Mexican
648 Pacific, Marine Micropaleontology, 66, 103-119.

649
650 McGillicuddy, Jr., D.J., Robinson, A.R., Siegel, D.A., Jannasch, H.W., Johnson, R.,
651 Dickey, T.D., McNeil, J., Michaels, A.F., Knap, A.H., 1998. Influence of mesoscale
652 eddies on new production in the Sargasso Sea. Nature, 394, 263-266.
653
654 McGillicuddy, Jr, D.J., Jonhson, R., Siegel, D.A., Michaels, A.F., Bates, N.R., Knap,
655 A.H., 1999. Mesoscale variations of biogeochemical properties in the Sargasso Sea,
656 Journal of Geophysical Research, 104, C6, 13 381-13 394.
657
658 McGillicuddy D.J., Anderson, L., Bates, N.R., Bibby, T., Buesseler, K.O., Carlson,
659 C.S., Davis, C., Ewart, P.G., Flakowski, S.A., Goldthwait, D., Hansell, Jenkins, W.J.,
660 Johnson, R., Kosnyrev, V.K., Ledwell, J., Li, Q., Siegel, D., Steinberg, D.K., 2007.
661 Eddy/Wind interactions stimulate extraordinary mid-ocean plankton blooms. Science,
662 316, 1021-1025.
663
664 McNeil, J.D., Jannasch, H.W., Dickey, T., McGillicuddy, D., Brzezinski, M.,
665 Sakamoto, C.M., 1999. New chemical, bio-optical and physical observations of upper

666 ocean response to the passage of a mesoscale eddy off Bermuda. Journal of
667 Geophysical Research, 104, 15 537-15 548.
668
669 Menzel, D.W., Ryther, 1961. Annual variations in primary production of the
670 Sargasso Sea off Bermuda. Deep-Sea Research, 7, 282-288.
671
672 Michaels A.F., Knap, A.H., Dow, R.L., Gundersen, K., Johnson, R.J., Sorensen, J.,
673 Close, A., Knauer, G.A., Lohrenz, S.E., Asper, V.A., Tuel, M., Bidigare, R., 1994.
674 Seasonal patterns of ocean biogeochemistry at the U.S. JGOFS Bermuda Atlantic
675 Time-series Study site. Deep-Sea Research I, 41, 1013-1038.
676
677 Michaels, A.F., Knap, A.H., 1996. Overview of the U.S.JGOFS BATS and
678 Hydrostation S program. Deep-Sea Research II, 43, 157-198.
679
680 Mouriño-Carballido, B., McGillicuddy, D.J., (2006) Mesoscale variability in the
681 metabolic balance of the Sargasso Sea, Limnology and Oceanography, 51, 2675-2689
682
683 Nelson, N.B., Siegel, D.A., Yoder, J.A., 2004. The spring bloom in the northwestern
684 Sargasso Sea: spatial extent and relationship with winter mixing. Deep-Sea Research
685 II, 51, 987-1000.
686
687 Northcote, L.C., Neil, H.L., 2005. Seasonal variations in foraminiferal flux in the
688 Southern Ocean, Campbell Plateau, New Zealand. Marine Micropaleontology, 56,
689 122-137
690
691 Olaizola, M., Ziemann, D.A., Bienfang, P.K., Walsh, W.A., Conquest, L.D., 1993.
692 Eddy-induced oscillations of the pycnocline affect the floristic composition and depth
693 distribution of phytoplankton in the subtropical Pacific. Marine Biology, 116, 533-
694 542.
695
696 Oschlies, A., and Garçon, V., 1998. Eddy-induced enhancement of primary
697 production in a model of the North Atlantic Ocean, Nature, 394, 266-269.

698
699 Oschlies, A., 2001. NAO-induced long-term changes in nutrient supply to the surface
700 waters of the North Atlantic. Geophysical Research Letters, 28, 1751-1754.
701
702 Oschlies, A., 2002. Can eddies make ocean deserts bloom? Global Biogeochemical
703 Cycles, 16, 1106.
704
705 Palter, J.B., Lozier, M.S., Barber, R.T., 2005. The effect of advection on the nutrient
706 reservoir in the North Atlantic subtropical gyre, Nature, 437, 687-692.
707
708 Patara, L., Visbeck, M., Masina, S., Krahmann, G., Vichi, M., 2011. Marine
709 biogeochemical responses to the North Atlantic Oscillation in a coupled climate
710 model, Journal of Geophysical Research, 116, C07023.
711
712 Pujol, C., and Vergnaud Grazzini, C., 1995. Distribution patterns of live planktic
713 foraminifers as related to regional hydrography and productive systems of the
714 Mediterranean Sea, Marine Micropaleontology, 25, 187-217
715
716 Rodwell, M.J., Rowell, D.P., Folland, C.K., 1999. Oceanic forcing of the wintertime
717 North Atlantic Oscillation and European Climate. Nature, 398, 320-323.
718
719 Sautter, L., and Thunell, R.C., 1989. Seasonal succession of planktonic foraminifera:
720 Results from a four-year time series sediment trap experiment in the northeast Pacific,
721 Journal of Foraminiferal Research, 19, 253-267.
722
723 Schiebel, R., 2002. Planktic foraminiferal sedimentation and the marine calcite
724 budget, Global Biogeochemical Cycles, 16, 1065, doi:10.1029/2001GB001459
725
726 Schmuker B., and Schiebel, R., 2002. Planktic foraminifers and hydrography of the
727 eastern and northern Caribbean Sea, Marine Micropaleontology, 46, 387-403

Seki, M.P., Polovina, J.J., Brainard, R.E., Bidigare, R.R., Leonard, C.L., Foley, D.G., 2001. Biological enhancement at cyclonic eddies tracked with GOES thermal imagery in Hawaiian waters. Geophysical Research Letters, 28, 1583-1586.

Sexton, P.F. and Norris, R.D. (2008), Dispersal and biogeography of marine plankton: Long-distance dispersal of the foraminifer Truncorotalia truncatulinoides, Geology, 36, 899-902.

Sexton, P.F. and Norris, R.D. (2011), High latitude regulation of low latitude thermocline ventilation and planktic foraminifer populations across glacial-interglacial cycles, Earth and Planetary Science Letters, 311, 69-81.

Siegel, D.A., Doney, S.C., Yoder, J.A., 2002. The North Atlantic Spring Phytoplankton Bloom and Sverdrup's Critical Depth Hypothesis, Science, 296, 730-733.

Storz, D., Schulz, H., Waniek, J.J., Schulz-Bull, D.E., Kučera, M., 2009. Seasonal and interannual variability of the planktic foraminiferal flux in the vicinity of the Azores Current. Deep Sea Research I, 56, 107-124.

Spero, H.J., 1998. Life history and stable isotope geochemistry of planktonic foraminifera, In R.D. Norris and R. M. Corfield (eds.) *Isotope Paleobiology and Paleoecology*; Paleontological Society Papers. Special Publication.

Sprintall, J., Tomczak, M., 1992. Evidence of the barrier layer in the surface layer of the tropics. Journal of Geophysical Research: Oceans, 97, 7305-7316.

Steinberg, D.K., Carlson, C.A., Bates, N.R., Rodney, J.J., Michaels, A.F., Knap, A.H., 2001. Overview of the US JGOFS Bermuda Atlantic Time-series Study (BATS): a decade-scale look at ocean biology and biogeochemistry. Deep-Sea Research II, 48, 1405-1447.

761 Sweeney E.N., McGillicuddy, Jr, D.J., Buesseler, K.O., 2003. Biogeochemical
762 impacts due to mesoscale eddy activity in the Sargasso Sea as measured at the
763 Bermuda Atlantic Time-series Study (BATS). Deep-Sea Research II, 50, 3017-3039.
764
765 Takahashi, K., Bé, A.W.H., 1984. Planktonic foraminifera: factors controlling
766 sinking speed, Deep-Sea Research, 31, 1477-1500.
767
768 Thunell, R.C., and Reynolds, L.A., (1984) Sedimentation of planktonic foraminifera:
769 seasonal changes in species flux in the Panama Basin, Micropaleontology, 30, 243-
770 262.
771
772 Tolderlund, D.S., Bé, A.W.H., 1971. Seasonal distribution of planktonic foraminifera
773 in the western North Atlantic. Micropaleontology 17, 297-329.
774
775 Townsend, D.W., Cammen, L.M., Holligan, P.M., Campbell, D.E., Pettigrew, N.R.,
776 1994. Causes and consequences of variability in the timing of spring phytoplankton
777 blooms. Deep-Sea Research I 41, 747-765.
778
779 Treusch, A.H., Demir-Hilton, E., Vergin, K.L., Worden, A.Z., Carlson, C.A., Donatz,
780 M.G., Burton, R.M., Giovannoni, S.J., (2012) Phytoplankton distribution patterns in
781 the northwestern Sargasso Sea revealed by small subunit rRNA genes from plastids,
782 ISME Journal, 6, 481-492
783
784 Waniek, J.J., 2003. The role of physical forcing in initiation of spring blooms in the
785 northeast Atlantic. Journal of Marine Systems, 39, 57-82.
786
787 Wiebe, P.H., Joyce, T., 1992. Introduction to interdisciplinary studies of Kuroshio
788 and Gulf Stream rings. Deep-Sea Research Part A, Oceanographic Research Papers,
789 39, supplement 1, 5-6.
790
791 Žarić, S., Donner, B., Fischer, G., Mulitza, S., Wefer, G., 2005. Sensitivity of
792 planktic foraminifera to sea surface temperature and export production as derived
793 from sediment trap data. Marine Micropaleontology, 55, 75-105.

794
795 Zeebe, R.E., Bijma, J., Hoenisch, B., Sanyal, A., Spero, H.J., Wolf-Gladrow, D.A.,
796 2008. Vital Effects and Beyond: A Modeling Perspective on Developing
797 Paleoceanographic Proxy Relationships in Foraminifera. The Geological Society,
798 London. Special Publications, 303, 45-58. Biogeochemical Controls on
799 Palaeoceanographic Proxies. Eds.: James, R., Austin, W. E. N., Clarke, L., Rickaby, R.
800 E. M.
801

802 **Figure Captions**

803 **Figure 1.** Map to show locations of the Oceanic Flux Program (OFP) mooring
804 (31°50'N, 64°10'W) and the Bermuda Atlantic Time Series (BATS) hydrographic
805 station (31°50'N, 64°10'W) and Seasonal Changes in Foraminifera Flux (SCIFF) site
806 and Hydrostation S in relation to Bermuda Island.
807
808 **Figure 2.** Temporal changes in total planktonic foraminifera flux and mass,
809 carbonate, and organic carbon fluxes at 1500 m depth over the six year study period.
810
811 **Figure 3.** Temporal changes in environmental parameters measured at the BATS site
812 in relation to total planktic foraminiferal flux in the 1500m OFP trap (thin, black line)
813 a) Sea surface temperature (0-25 m), b) Sea level height anomaly; grey bars indicate
814 periods when productive cyclonic eddies influenced the site, c) Mixed layer depth, d)
815 Chlorophyll *a* concentration (0-25 m average) e) Average organic carbon flux at 200
816 m
817
818 **Figure 4.** Correlation between total planktonic foraminifera flux in the 1500 m OFP
819 trap (thin, black line) with environmental parameters measured at the BATS site. a)
820 Chlorophyll *a* concentration at 0-25 m. The correlation excludes an anomalous peak
821 in chlorophyll *a* concentration observed in 2010. b) MLDs >80 m, excluding the
822 extremely deep MLD observed in 2010. c) MLDs <80 m.
823
824 **Figure 5.** Temporal changes in surface dwelling planktic foraminifera fluxes in the
825 1500m trap with changes in sea surface temperature (0-25 m) shown in the dashed

826 black line for reference. The approximate depth habitat (Anand et al. 2003) is shown
827 on figures.
828
829 **Figure 6.** Temporal changes in intermediate dwelling planktonic foraminifera fluxes
830 in the 1500 m trap with changes in sea surface temperature (0-25 m) for reference.
831 The approximate depth habitat (Anand et al. 2003) is shown on figures.
832
833 **Figure 7.** Temporal changes in deeper dwelling planktonic foraminifera fluxes in the
834 1500 m trap with changes in sea surface temperature (0-25 m) for reference. The
835 approximate depth habitat (Anand et al. 2003) is shown on figures. Graphs are
836 ordered according to seasonal succession.
837
838 **Figure 8.** Seasonal succession for deeper dwelling species averaged over six spring
839 blooms (1998, 1999, 2000, 2008, 2009, 2010) from the 1500 m trap. *G.*
840 *truncatulinoides, G. hirsuta, G. inflata* appear on the left axis and *G. crassaformis* is
841 on the right axis..
842
843 **Figure 9.** a) The relative contribution of total PF to total carbonate flux b) The
844 relative contribution of deeper dwelling planktonic foraminifera (*G. hirsuta, G.*
845 *truncatulinoides, G. crassaformis, G. inflata)* to the total planktonic foraminiferal
846 carbonate flux c) The relative contribution of total deeper dwellers (*G. hirsuta, G.*
847 *truncatulinoides, G. crassaformis, G. inflata*) to the total carbonate flux. All graphs
848 show four full years 1998-99, 1999-00, 2008-09 and 2009-10.
849

Figure 10. a) Correlation between the maximum mixed layer depth and deepening rate of the mixed layer for years 1995-2011. Correlation between the deepening:sholaing rate (D_r/S_r) ratio of the mixed layer depth for all years studies excluding 2000 and b) Integrated PF flux during the spring blooms which ranged from Dec-May c) maximum chlorophyll *a* concentrations in the surface ocean during the spring bloom for all years studied, excluding the anomalous year 2010 in parentheses d) Correlation between the shoaling rate and integrated flux of total PF over the spring bloom period which ranged from Dec-May. Diamonds indicate years with eddy influence 2009 and diamond with parentheses = 2010. Round points are years without eddy influence.

Figure 11. Annual integrated PF flux from this study (1500m trap, square symbols) and 1979-1984 (*3200m trap, round symbols, Deuser, 1987, Deuser and Ross, 1989) plotted against wintertime (DJFM) NAO index + 1 year lag. Annual fluxes from both trap depths are comparable. **Annual PF flux from 1978 (diamond symbol) was not included in the regression because it was an anomalously low flux year which could be explained by a shallow MLD and/or possibly the presence of an anticyclonic eddy (no data to test), which may have suppressed the spring bloom and hence PF flux as seen during 1994 at BATS (Lomas et al. 2013). NAO data available from http://www.cpc.ncep.noaa.gov/data/teledoc/nao.shtml

872 Table 1. Annual fluxes for planktonic foraminifera species at 1500 m depth in 1998-1999, 1999-2000, 2008-2009 and 2009-2010 and the four-
873 year averages. Fluxes were calculated from the sum of biweekly averages between July-June for each year and converted to tests m^{-2} yr^{-1}.
874 Species are listed according to their estimated depth habitats.

		Annual flux (tests m^{-2} yr^{-1})					
Species	Seasonal flux maximum	1998-1999	1999-2000	2008-2009	2009-2010	Average	3200m avg (1978-1984)[3]
Surface dwellers:							
G. ruber (pink)	July-Sept	2524	1978	1576	2122	2050	1450
G. ruber (white)	Sept-Oct	16 197	19 633	13 917	18 719	17 117	
G. sacculifer	Oct[1]. March[2]	256	292	1007	348	1903	425
Surface Totals		18 977	21 903	16 500	21 189	17 346	
Intermediate dwellers:							
G. siphonifera	*	6101	3182	2231	2833	3587	
O. universa	April-May[1], Oct-Nov[2]	1429	694	1056	2250	1357	
G. conglobatus	Nov	277	180	0	4	115	300
N. dutertrei	March-April[1], Nov-Dec[2]	1290	185	471	839	696	876
P. obliquiloculata	Dec-March	398	205	708	352	416	762
Intermediate Totals		9495	4446	4466	6278	6171	
Deep dwellers:							
G. truncatulinoides	Jan-Feb	5248	13 796	9517	4031	8148	3420
G. hirsuta	Feb-March	1784	9888	3859	2770	4575	1520
G. crassaformis	Feb-March	26	100	122	139	97	192
G. inflata	March-April	844	995	1652	1869	1340	1270
Deep Totals		7902	24 779	15 150	8809	14 160	5402
Other species	-	51 442	43 704	43 172	70 446	51 191	
Totals	-	87 816	94 831	79 289	106 722	92 165	

875 [1] Primary peak
876 [2] Secondary peak
877 [3] Averages from Deuser and Ross, 1989
878 * This species has low seasonality

879 Table 2. Mixed layer depth and mean rates of mixed layer (ML) deepening and shoaling. The D_r/S_r ratio is a derived value calculated from the
880 rate of ML deepening divided by the rate of ML shoaling (see text). The winter-spring PF flux represents the PF flux integrated over the whole
881 bloom, which varied interannually in length but ranged from Dec-May. Shaded years indicate years when a cyclonic eddy was present during
882 the spring bloom period.
883
884

Year	MLD max (m)	ML Deepening Rate (m day^{-1})	ML Shoaling Rate (m day^{-1})	D_r/S_r ratio (m)	Maximum PF flux (tests m^{-2} day^{-1})	Integrated winter-spring PF flux (tests m^{-2} day^{-1})
1997-1998	235	0.93	1.91	0.49	641	28
1998-1999	222	0.78	7.78	0.10	816	41
1999-2000	197	0.63	Data missing	-	761	30
2007-2008	130	0.55	0.75	0.73	385	17
2008-2009	198	0.95	2.21	0.43	946	28
2009-2010	464	1.76	3.82	0.46	815	32

885

Fig.01

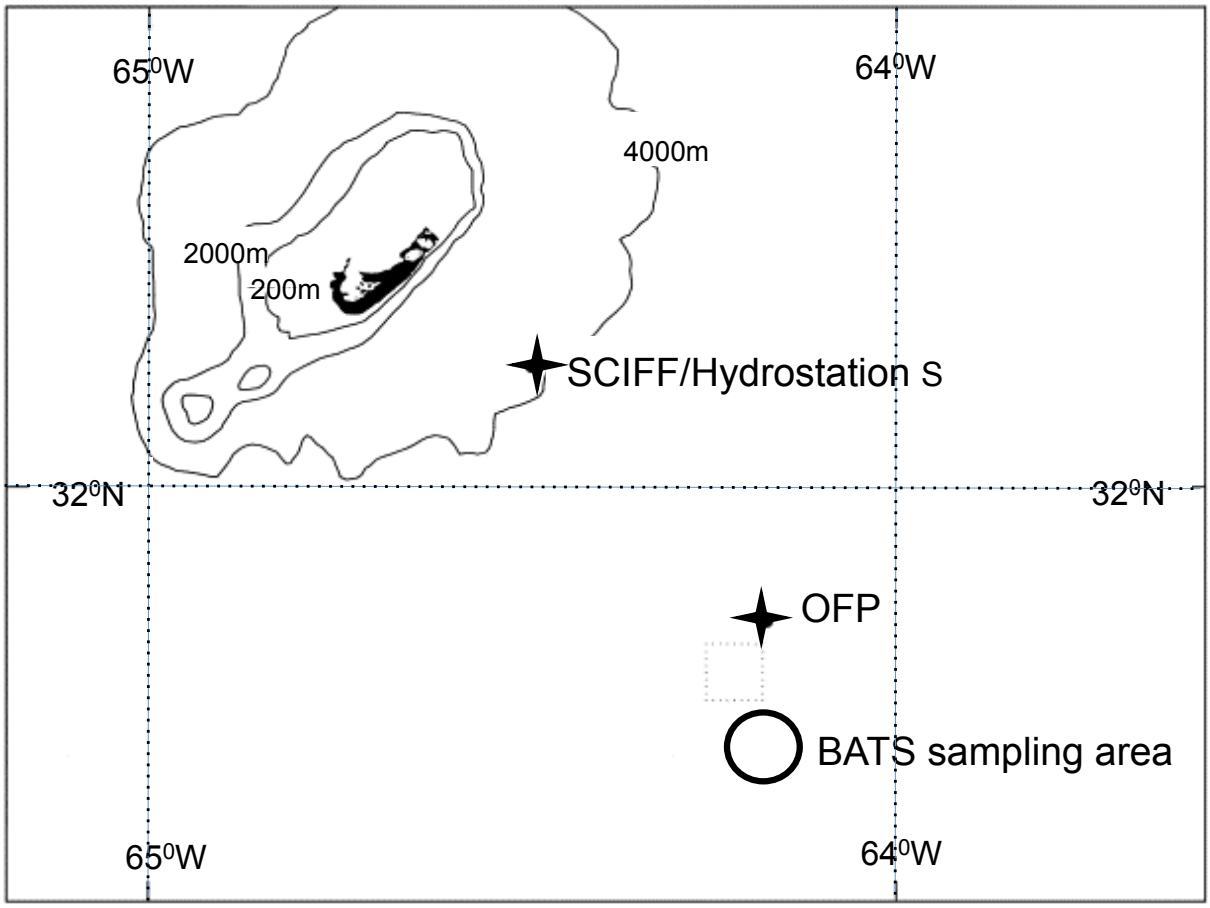
65⁰W
64⁰W
4000m
2000m
200m
SCIFF/Hydrostation S
32⁰N
32⁰N
OFP
BATS sampling area
65⁰W
64⁰W

Fig.02

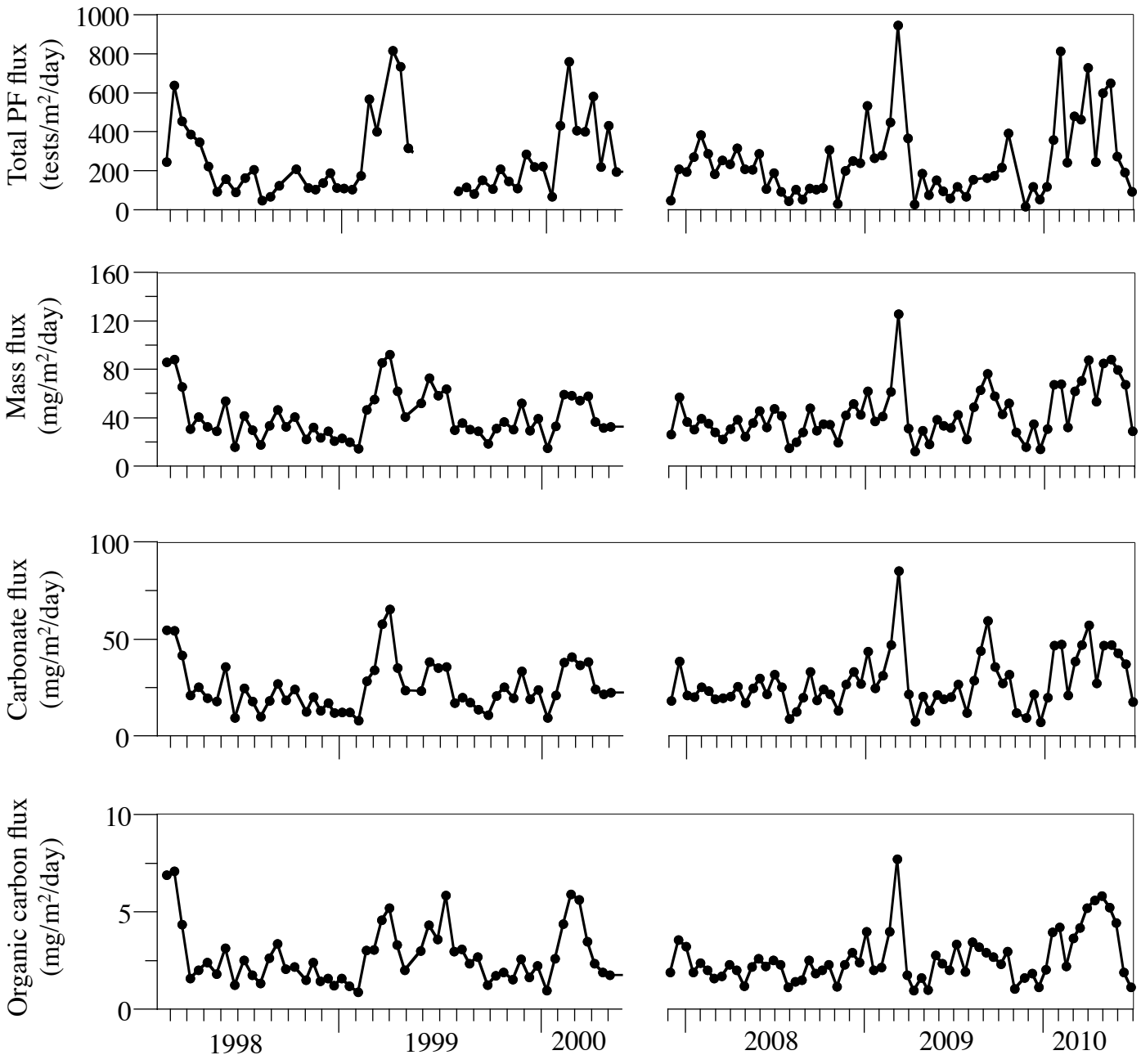
Total PF flux (tests/m2/day)
1000
800
600
400
200
0
Mass flux (mg/m2/day)
160
120
80
40
0
Carbonate flux (mg/m2/day)
100
50
0
Organic carbon flux (mg/m2/day)
10
5
0
1998
1999
2000
2008
2009
2010

Fig.03

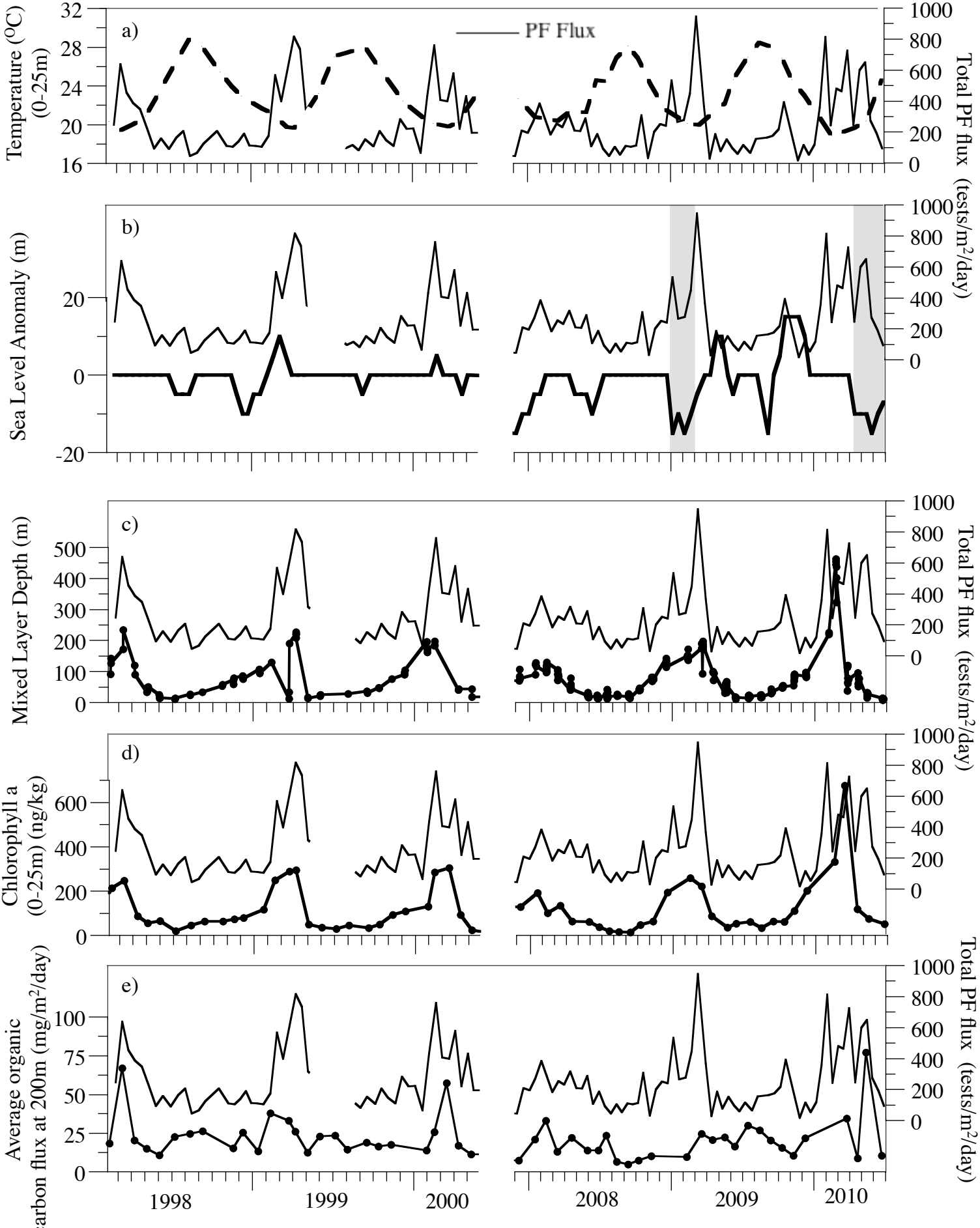
a)
PF Flux
Temperature (°C) (0-25m)
Total PF flux (tests/m²/day)
b)
Sea Level Anomaly (m)
c)
Mixed Layer Depth (m)
d)
Chlorophyll a (0-25m) (ng/kg)
e)
Average organic carbon flux at 200m (mg/m²/day)
1998
1999
2000
2008
2009
2010

Fig.04

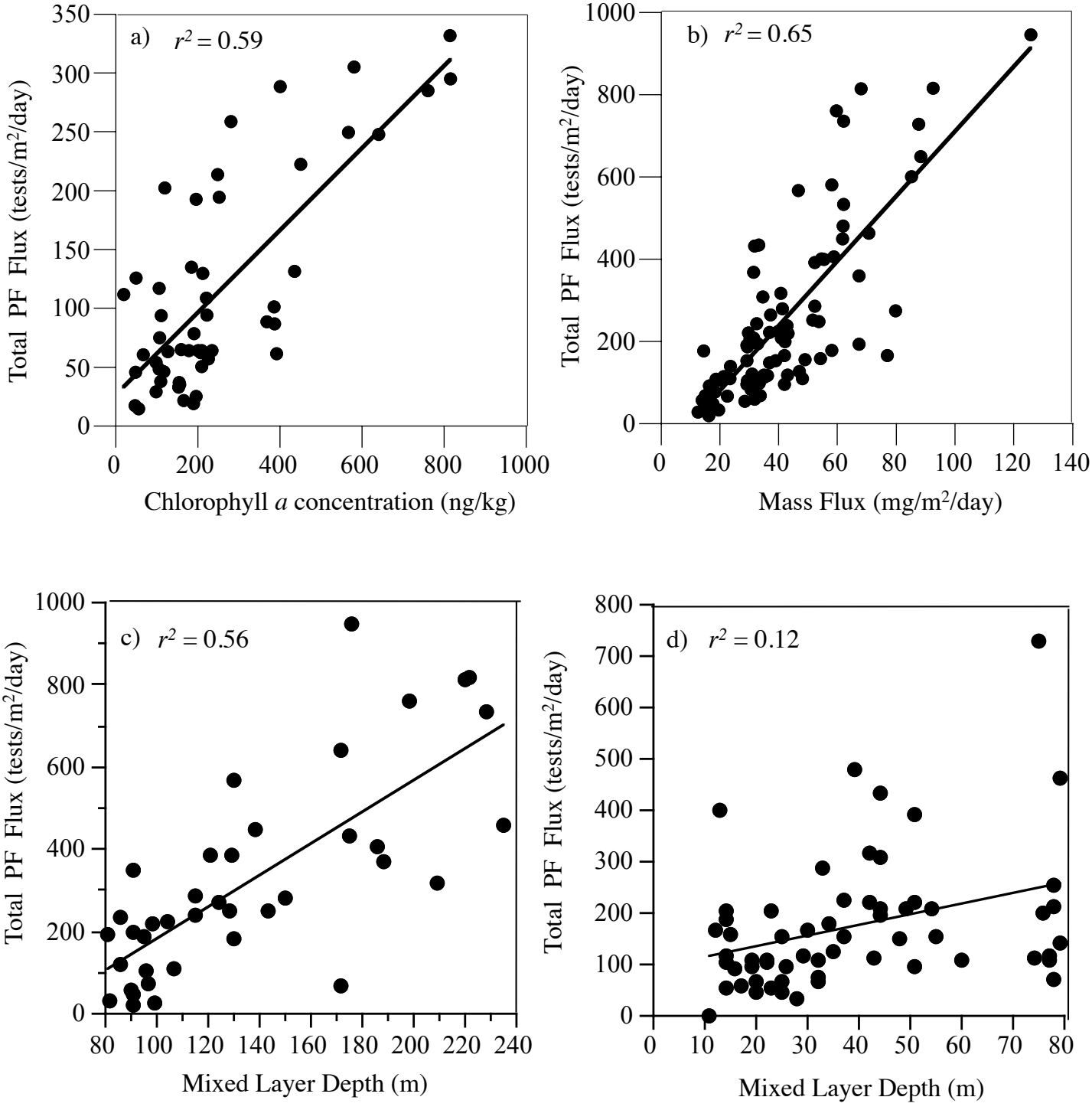
a) $r^2 = 0.59$
Total PF Flux (tests/m^2/day)
Chlorophyll *a* concentration (ng/kg)
b) $r^2 = 0.65$
Total PF Flux (tests/m^2/day)
Mass Flux (mg/m^2/day)
c) $r^2 = 0.56$
Total PF Flux (tests/m^2/day)
Mixed Layer Depth (m)
d) $r^2 = 0.12$
Total PF Flux (tests/m^2/day)
Mixed Layer Depth (m)

Fig.05

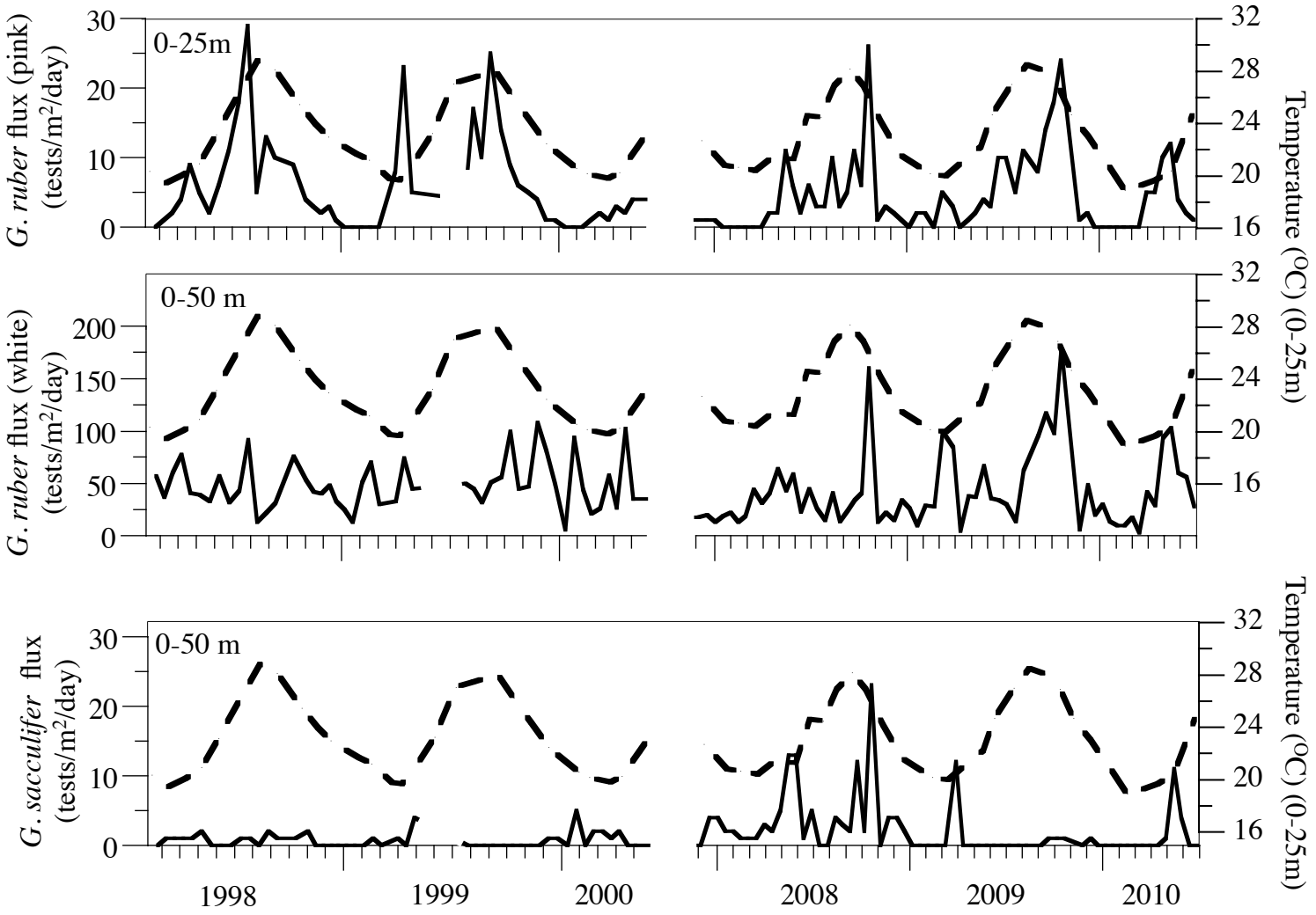
0-25m
G. ruber flux (pink) (tests/m2/day)
Temperature (°C) (0-25m)
0-50 m
G. ruber flux (white) (tests/m2/day)
0-50 m
G. sacculifer flux (tests/m2/day)
1998
1999
2000
2008
2009
2010

Fig.06

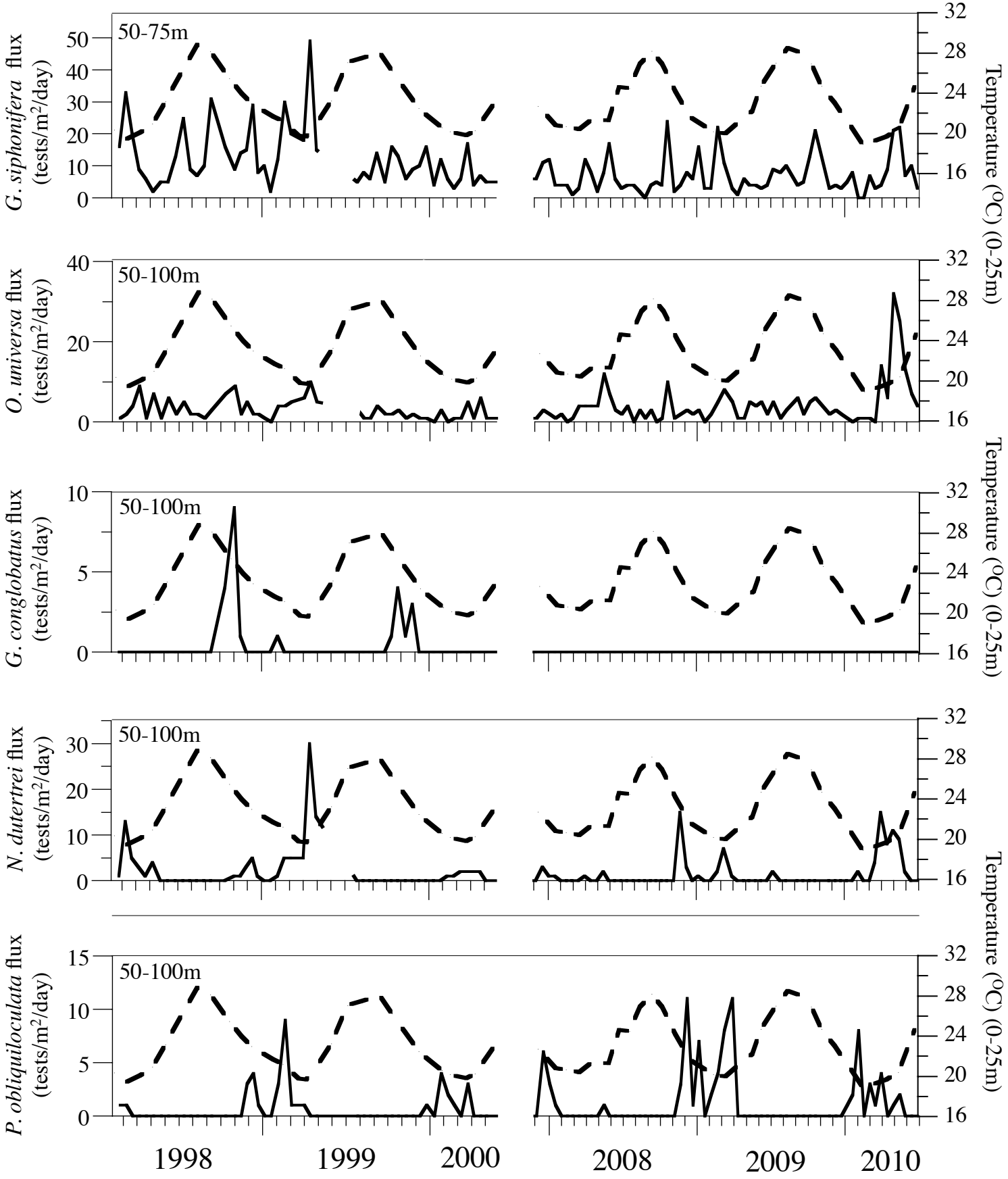
50-75m
50-100m
50-100m
50-100m
50-100m
G. siphonifera flux (tests/m²/day)
O. universa flux (tests/m²/day)
G. conglobatus flux (tests/m²/day)
N. dutertrei flux (tests/m²/day)
P. obliquiloculata flux (tests/m²/day)
Temperature (°C) (0-25m)
1998
1999
2000
2008
2009
2010

Fig.07

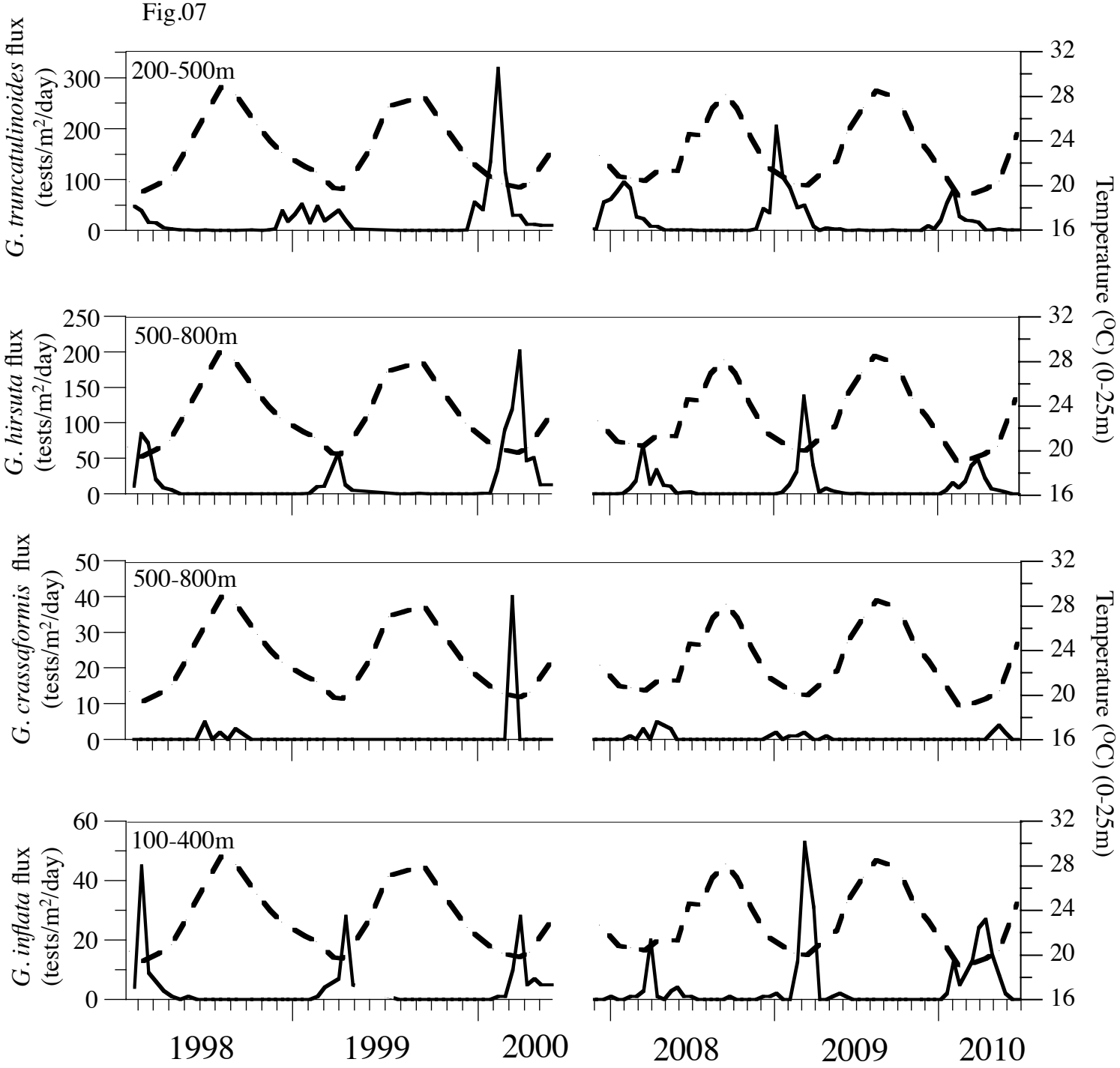
G. truncatulinoides flux (tests/m²/day)
200-500m
G. hirsuta flux (tests/m²/day)
500-800m
G. crassaformis flux (tests/m²/day)
500-800m
G. inflata flux (tests/m²/day)
100-400m
Temperature (°C) (0-25m)
1998
1999
2000
2008
2009
2010

Fig.08

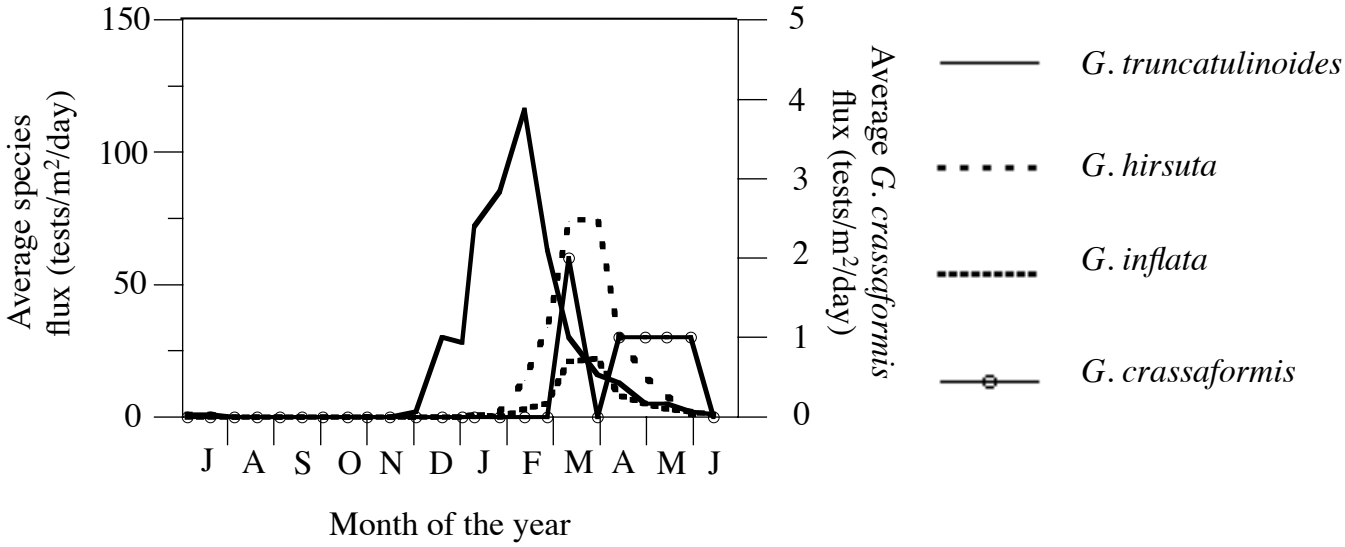
150
100
50
0
5
4
3
2
1
0
J A S O N D J F M A M J
Month of the year
Average species flux (tests/m²/day)
Average G. crassaformis flux (tests/m²/day)
G. truncatulinoides
G. hirsuta
G. inflata
G. crassaformis

Fig.09

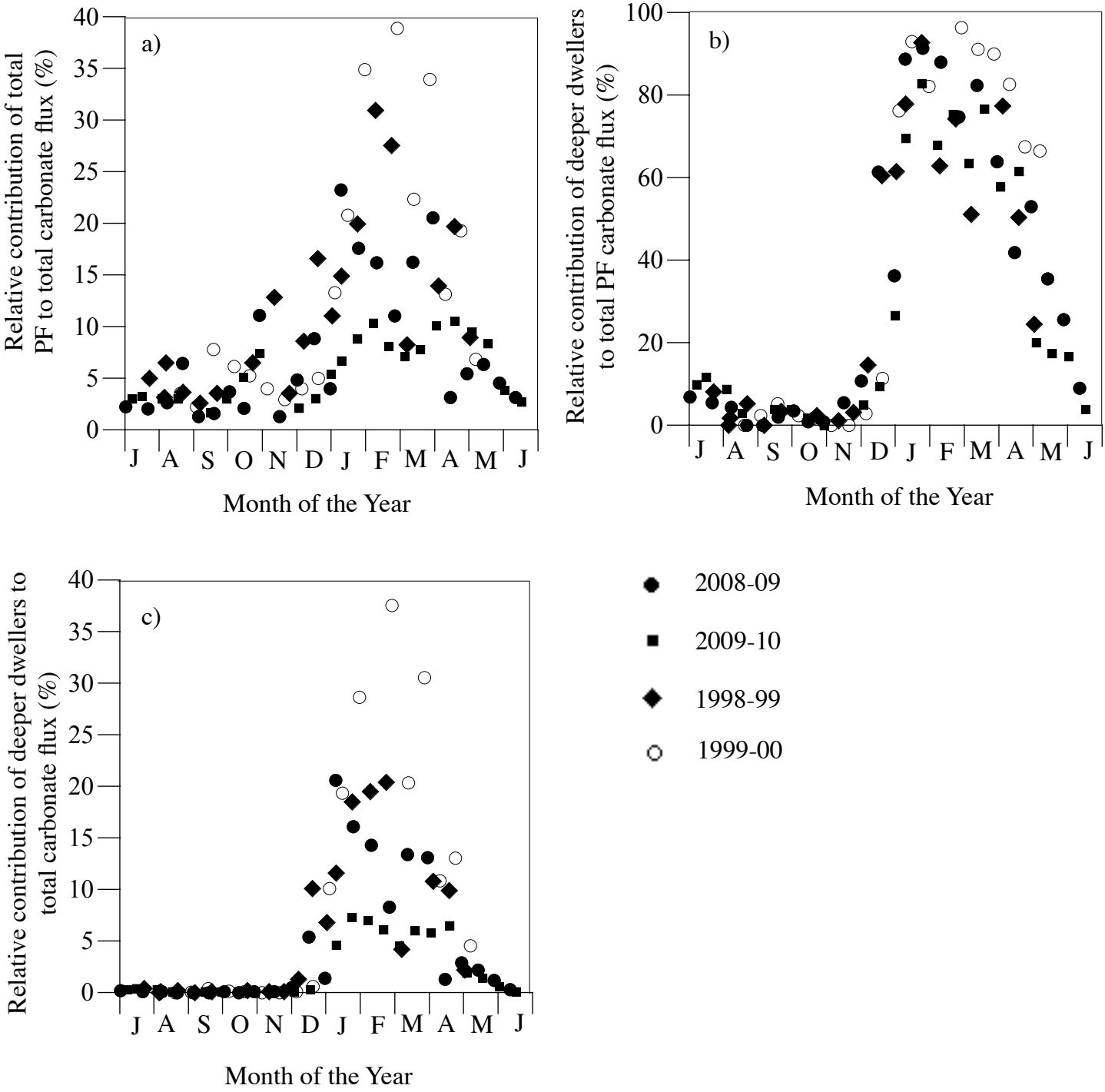
a)
Relative contribution of total PF to total carbonate flux (%)
0
5
10
15
20
25
30
35
40
J A S O N D J F M A M J
Month of the Year
b)
Relative contribution of deeper dwellers to total PF carbonate flux (%)
0
20
40
60
80
100
J A S O N D J F M A M J
Month of the Year
c)
Relative contribution of deeper dwellers to total carbonate flux (%)
0
5
10
15
20
25
30
35
40
J A S O N D J F M A M J
Month of the Year
2008-09
2009-10
1998-99
1999-00

Fig.10

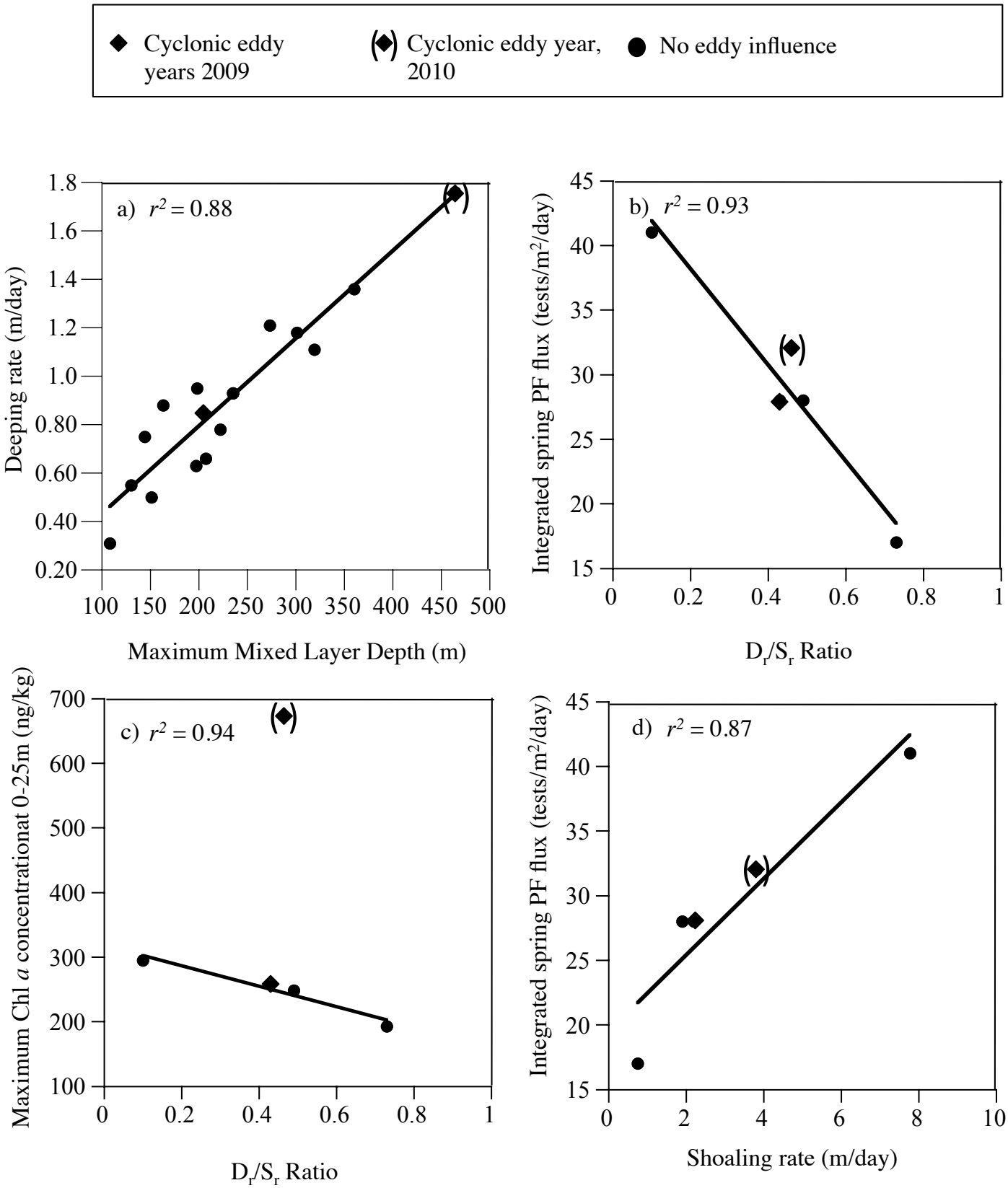
Cyclonic eddy years 2009
Cyclonic eddy year, 2010
No eddy influence
a) $r^2 = 0.88$
Deeping rate (m/day)
Maximum Mixed Layer Depth (m)
b) $r^2 = 0.93$
Integrated spring PF flux (tests/m^2/day)
D_r/S_r Ratio
c) $r^2 = 0.94$
Maximum Chl *a* concentrationat 0-25m (ng/kg)
D_r/S_r Ratio
d) $r^2 = 0.87$
Integrated spring PF flux (tests/m^2/day)
Shoaling rate (m/day)

Fig.11

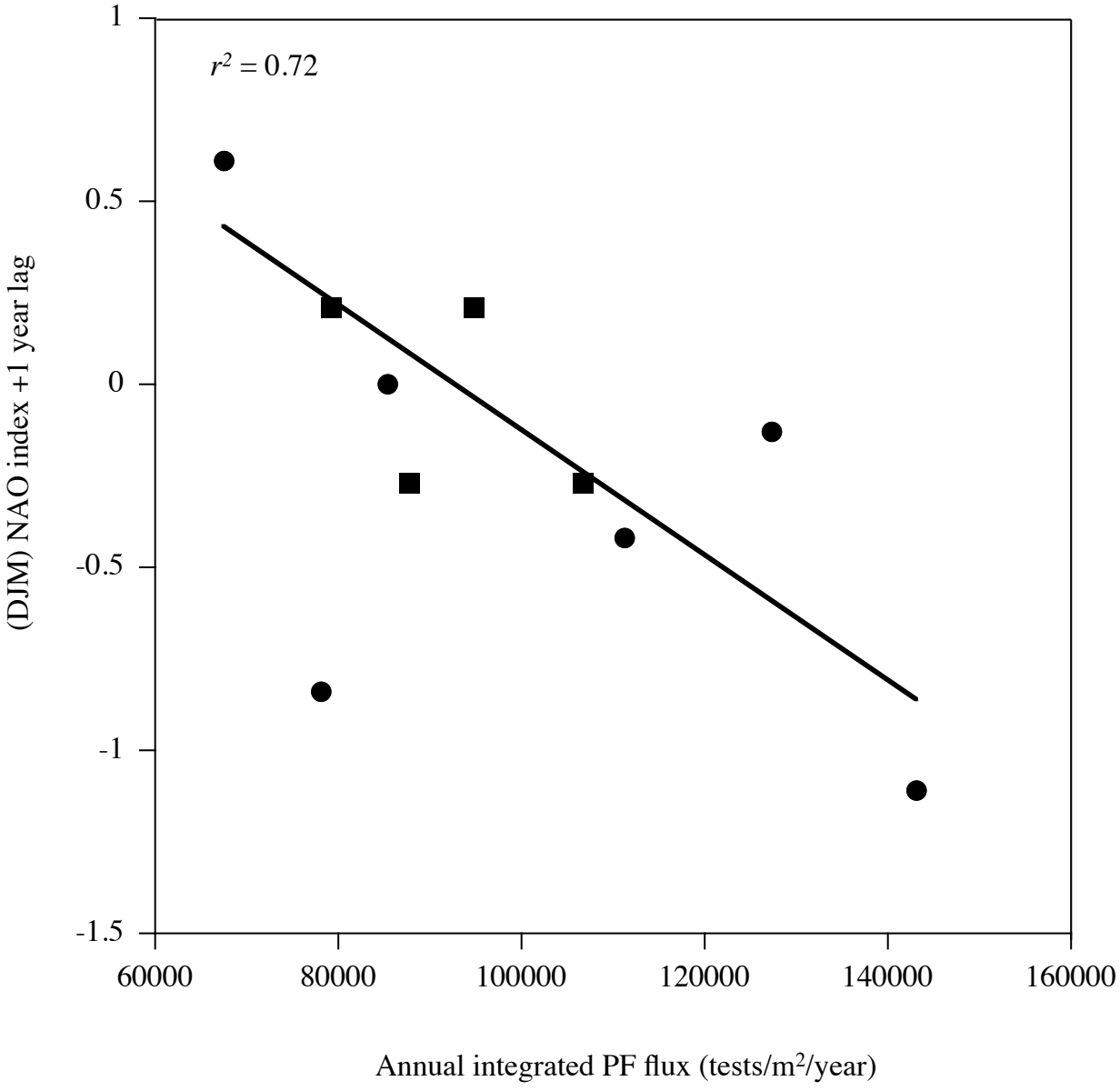
r^2 = 0.72
1
0.5
0
-0.5
-1
-1.5
60000
80000
100000
120000
140000
160000
(DJM) NAO index +1 year lag
Annual integrated PF flux (tests/m^2/year)